



RESEARCH ARTICLE

Numerical study of osteophyte effects on preoperative knee functionality in patients undergoing total knee arthroplasty

Periklis Tzanetis¹  | Kevin de Souza² | Seonaid Robertson² | René Fluit³  |
Bart Koopman¹ | Nico Verdonschot^{1,4}

¹Department of Biomechanical Engineering, University of Twente, Enschede, The Netherlands

²Stryker, Manchester, UK

³Faculty of Science and Engineering, University of Groningen, Groningen, The Netherlands

⁴Orthopaedic Research Laboratory, Radboud Institute for Health Sciences, Radboud University Medical Center, Nijmegen, The Netherlands

Correspondence

Periklis Tzanetis, Department of Biomechanical Engineering, University of Twente, De Horst 2, 7522 LW, Enschede, The Netherlands.
Email: p.tzanetis@utwente.nl

Funding information

Stryker European Operations Ltd., Ireland

Abstract

Osteophytes are routinely removed during total knee arthroplasty, yet the preoperative planning currently relies on preoperative computed tomography (CT) scans of the patient's osteoarthritic knee, typically including osteophytic features. This complicates the surgeon's ability to anticipate the exact biomechanical effects of osteophytes and the consequences of their removal before the operation. The aim of this study was to investigate the effect of osteophytes on ligament strains and kinematics, and ascertain whether the osteophyte volume and location determine the extent of this effect. We segmented preoperative CT scans of 21 patients, featuring different osteophyte severity, using image-based active appearance models trained to identify the osteophytic and preosteophytic bone geometries and estimate the cartilage thickness in the segmented surfaces. The patients' morphologies were used to scale a template musculoskeletal knee model. Osteophytes induced clinically relevant changes to the knee's functional behavior, but these were variable and patient-specific. Generally, severe osteophytic knees significantly strained the oblique popliteal ligament (OPL) and posterior capsule (PC) relative to the preosteophytic state. Furthermore, there was a marked effect on the lateral collateral ligament and anterolateral ligament (ALL) strains compared to mild and moderate osteophytic knees, and concurrent alterations in the tibial lateral-medial translation and external-internal rotation. We found a strong correlation between the OPL, PC, and ALL strains and posterolateral condylar and tibial osteophytes, respectively. Our findings may have implications for the preoperative planning in total knee arthroplasty, toward reproducing the physiological knee biomechanics as close as feasibly possible.

KEYWORDS

musculoskeletal modeling, osteophytes, preosteophytic bones, total knee arthroplasty

This is an open access article under the terms of the [Creative Commons Attribution](https://creativecommons.org/licenses/by/4.0/) License, which permits use, distribution and reproduction in any medium, provided the original work is properly cited.

© 2024 The Authors. *Journal of Orthopaedic Research*® published by Wiley Periodicals LLC on behalf of Orthopaedic Research Society.

1 | INTRODUCTION

Osteophyte formation is one of the main pathological features of knee osteoarthritis (OA) and an important criterion in assessing the development and progression of disease.¹ To date, several studies support the hypothesis that osteophytes develop in response to excessive mechanical loads as an attempt to reduce stress on the OA joint, redistributing the forces to a larger articulating surface.^{2,3} Osteophytes are also thought to arise from a bone remodeling process secondary to pathological joint alterations, such as anteriorly to the tibial plateau in case of a ruptured anterior cruciate ligament, to prevent anteroposterior instability.⁴ Concomitantly, the formation of osteophytes may restrict the range of joint motion and, subsequently, cause a pathological deformity, depending on the characterized size and direction of osteophytes⁵ as well as the osteophytic compartment.⁶ Previous research suggests that large posterior condylar osteophytes prevent terminal knee extension due to increased tension of the posterior capsule, thus contributing to adjacent ligamentous imbalance.⁷ One longitudinal study found that large medial tibial osteophytes are present in varus knees.⁸ This tightens the medial ligamentous structures increasing asymmetric loading in the medial compartment. Intuitively, osteophytes on the lateral side of the tibial plateau would likely have the opposite loading effect.

During total knee arthroplasty, surgeons routinely remove the osteophytes toward achieving restoration of more physiological knee biomechanics⁹; failure to remove them may result in unequal mediolateral flexion and extension gaps, hence soft-tissue imbalance,⁷ with consequent aberrant joint kinematics. Nevertheless, the preoperative planning phase of this operation remains guided by the preoperative computed tomography (CT) scan of the OA knee, commonly including osteophytic features, which complicates the surgeon's capacity to anticipate the precise biomechanical consequences of their removal before surgery. With established image-based, active appearance modeling techniques, it becomes possible to utilize the preoperative image of the OA knee and virtually reconstruct the knee bone shapes as before the growth of osteophytes,^{10–12} referred to here as the preosteophytic state. This research paper does not address total knee arthroplasty, but rather elaborates on the possible effects of osteophytes on the knee's biomechanical behavior, in relation to knees without osteophytes. Such biomechanical information could be comprehensively assessed using computational models of the musculoskeletal system; these can incorporate patient-specific bone geometries and enable to study the osteophyte effects on ligament strains and knee kinematics,¹³ and therefore, could possibly benefit the preoperative planning phase before the surgical execution. The ultimate importance of this work lies in the utilization of such musculoskeletal simulations in the preoperative planning of total knee arthroplasty.

The aim of this study was, therefore, first to investigate differences in ligament strains and knee kinematics between OA knees with different stages of osteophyte formation and their corresponding preosteophytic state; and, second, to explore whether

the volume and location of the osteophytes affect the extent of these biomechanical differences. We hypothesized that the presence of osteophytes would affect the strains of the ligaments and the consequent kinematic predictions, and the extent of this effect would depend on the volume and location of the osteophytes determining their interaction with the surrounding ligamentous structures. Confirmation of this hypothesis may have implications for the preoperative planning in total knee arthroplasty toward restoring physiological knee biomechanics as much as possible.

2 | METHODS

A template cadaver-specific musculoskeletal knee model was developed in the AnyBody Modeling System (AnyBody Technology A/S) based on CT and magnetic resonance images (MRI) of a male cadaveric lower extremity specimen (age 63, height 191 cm, body weight 87.5 kg), following a previously established methodology¹³; the resulting model served as the reference template model for subsequent personalization to the patient-specific data.¹⁴ This model comprises the thigh, shank, and patella. The knee is simulated to passively extend under gravity from 60° to 0°. The knee flexion angle is driven using a kinematic motion driver, while the remaining five degrees of freedom at the tibiofemoral joint equilibrate under the effect of muscle, ligament, and joint contact forces using the force-dependent kinematics approach.¹⁵ The selected range of motion is particularly important in gait,¹⁶ and limitations in knee function within this range are likely to affect the overall mobility of the OA patient. The patellofemoral joint was modeled as an idealized revolute joint, allowing only one translational degree of freedom of the patella controlled by an elastic patellar tendon, similar to an earlier study.¹⁷ The coordinates of quadriceps muscle attachments were determined from the MRI data set, and the Hill-type muscle-tendon element properties were adjusted to the Twente Lower Extremity Model 2.0 (TLEM 2.0).¹⁸ Ligaments were included to provide stability to the unconstrained tibiofemoral joint. A total of 27 nonlinear elastic spring elements were modeled to represent the anterior cruciate ligament (ACL), posterior cruciate ligament (PCL), deep medial collateral ligament (dmCL), superficial medial collateral ligament (smCL), lateral collateral ligament (LCL), anterolateral ligament (ALL), oblique popliteal ligament (OPL), and posterior capsule (PC). The individual ligament bundles could span from origin to insertion and find the shortest geodesic path to wrap around the femur and tibia, thereby preventing penetration into the bones. The attachment sites of knee ligaments were identified from the MRI; since the origins and insertions of the OPL and PC could not be determined from the data set, they were estimated according to anatomical descriptions found in the literature.¹⁹ Stiffness and reference strain assigned to the individual ligament bundles were originally adopted from the literature based on comparable intact knee models.^{13,20,21} Adjustments to the stiffness and reference strain of the ACL, PCL, OPL, and PC were made to ensure anteroposterior joint stability (Table 1), such that the overall tibial displacement relative to the femur during the

TABLE 1 Stiffness and reference strain of the individual ligament bundles used in the musculoskeletal knee model.

Ligament bundle	Stiffness (N) ^a	Reference strain ^b
Anteromedial ACL	2000	0.35
Posterolateral ACL	2000	0.35
Anterolateral PCL	1200	-0.46
Posteromedial PCL	1200	-0.03
Anterior dMCL	750	-0.17
Middle dMCL	750	-0.06
Posterior dMCL	750	-0.06
Anterior sMCL	2000	0.01
Middle sMCL	2000	0.01
Posterior sMCL	2000	0.01
Anterior LCL	2000	0.01
Middle LCL	2000	0.01
Posterior LCL	2000	0.01
Anterior ALL	2000	0.03
Posterior ALL	2000	0.03
OPL	4000	0.10
Medial PC	1000	0.07
Middle medial PC	1000	0.07
Middle lateral PC	1000	0.07
Lateral PC	1000	0.07

Abbreviations: ACL, anterior cruciate ligament; ALL, anterolateral ligament; dMCL, deep medial collateral ligament; LCL, lateral collateral ligament; OPL, oblique popliteal ligament; PC, posterior capsule; PCL, posterior cruciate ligament; sMCL, superficial medial collateral ligament.

^aStiffness is expressed in Newton (N) per unit strain.

^bReference strain refers to a fully extended knee position.

simulated knee extension motion remained within 4 mm anteriorly and 2 mm posteriorly,^{22,23} subjected to the influence of the gravitational force. The slack length of the ligament bundles was calibrated in a reference position in which the knee was fully extended.

The patient-specific data used in the present study were part of the knee functional flexion axis (FFA) data set.¹⁴ This anonymized data set includes preoperative CT scans of the lower extremity of 21 patients who underwent primary total knee arthroplasty using the Stryker Knee Navigation system (Stryker). The CT images of the individual patients were segmented to render the three-dimensional bone geometries of the hip, knee, and ankle joints. The bony structures of the knee were segmented using two different active appearance models (AAM), provided by Imorphics¹¹ (Stryker), that were trained on manual segmentations of CT images to identify the osteophytic femoral and tibial bone surfaces, as well as the bone surfaces beneath osteophytes,^{10,11} referred to as the preosteophytic bones (Figure 1). The osteophytic AAM was trained on a set of 670 cadaveric specimens with different stages of knee OA to detect osteophytes, which are typically visible along the periphery of the knee bones in OA subjects; the preosteophytic AAM was trained on manual segmentations of the osteophyte-free bone surfaces in a training set of 124 patient CT images. The accuracy of each model was assessed following a leave-one-out cross-validation procedure, comparing the model's output to the manually segmented ground truth surface; cross-validation involved repeatedly partitioning the data into training and test sets. Patients were equally assigned into three subgroups to stratify the severity of osteophyte formation according to the description of the previously established Kellgren-Lawrence (KL) classification system²⁴; KL-Grades 0 and 1 that refer to knees without osteophytes or doubtful osteophytic lipping, respectively, were not considered in the current convention, since our study included solely clinically confirmed osteophytic knees. The first subgroup included patients with definite knee osteophytes,

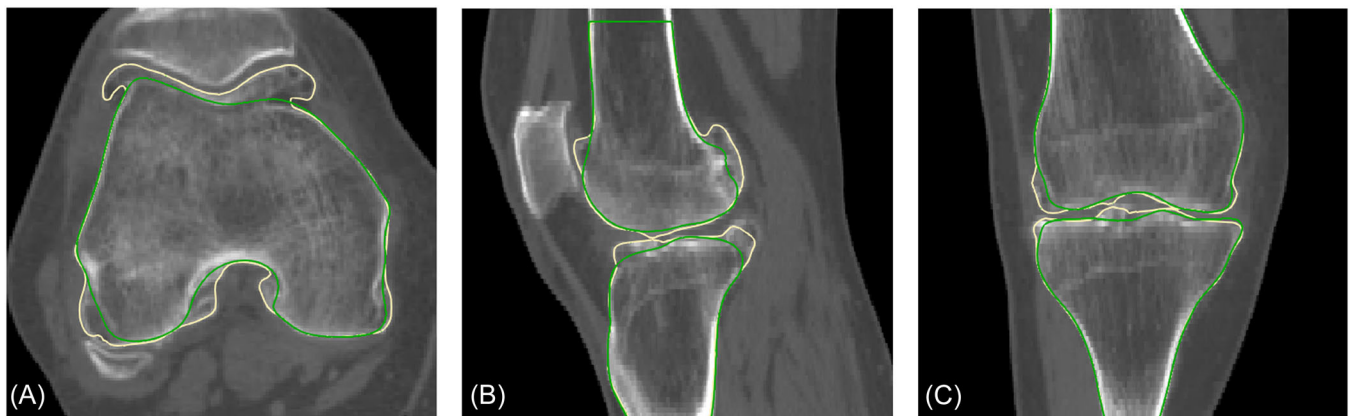


FIGURE 1 Computed tomography (CT) scan in axial (A), sagittal (B), and coronal (C) view of a single patient's knee depicting segmentation of the femoral and tibial osteophytic bones (yellow lines) and identification of the preosteophytic bone boundaries after removal of osteophytes (green line).

albeit of minimal severity (mild osteophytes), showing volumetric differences within 0–5 cm³ compared to the preosteophytic bones, corresponding to the criteria of KL-Grade 2. In the second subgroup, patients exhibited multiple moderate osteophytes, with volumetric differences within 5–10 cm³, and definite narrowing of the joint space, in consistency with KL-Grade 3. Patients allocated to the third subgroup demonstrated large osteophyte formation (severe osteophytes), measuring volumetric differences more than 10 cm³, severe narrowing of the joint space, and definite deformities of the femoral and tibial bone ends, aligned with KL-Grade 4. Figure 1 illustrates a representative severe case, which demonstrates large trochlear and posterior-compartment condylar and tibial osteophytes, narrowed joint space, and definite deformities of the femoral and tibial plateau ends. Osteophyte volumes were then generated per compartment, partitioning the femur and tibia into four regions: anterior medial, anterior lateral, posterior medial, and posterior lateral. For this, we used orthogonal planes derived from the transepicondylar axis and an anatomical landmark located at the central trochlea for the femur; and an axis connecting the medial and lateral proximal resection landmarks and the central tibia plateau landmark for the tibia (Figure 2). An MRI-based statistical shape model (SSM) approach was employed to estimate cartilage thickness from the bone surfaces segmented in CT on the basis of a previously published segmentation protocol.²⁵ More specifically, an SSM was trained on the combined bone and cartilage shapes segmented in MRI, utilizing a training set of 129 OA subjects. Subsequently, for each subject in the test or experimental set, we first segmented the bone-only surfaces in the CT image using the CT-based AAM described previously; and, second, given the patient-specific bone shape, we calculated the best-fitting instance of the combined bone and cartilage SSM.²⁶ A nonlinear scaling technique was employed to morph the topology of

the cadaveric bones to the patient-specific bones and subsequently the corresponding ligament attachments using a radial basis function interpolation scheme. This morphing technique has been described in previous studies.^{13,21} Anatomical coordinate systems for the femur, tibia, and patella were defined mapping selected bony landmarks at the hip and ankle segments, including the femoral head center and medial and lateral malleolus, in addition to the knee landmarks according to a previously defined measurement protocol.¹⁸ Specifically, the femoral coordinate system had its origin at the midpoint between the medial and lateral femoral epicondyles, and was oriented such that the y-axis pointing from the origin to the center of the femoral head, the z-axis was perpendicular to the y-axis pointing laterally, and the x-axis was perpendicular to both y- and z-axis pointing anteriorly. The origin of the tibial coordinate system was defined as the midpoint between the most medial and lateral points of the medial and lateral condyles of the tibia, respectively. The y-axis aligned with the line connecting the origin with the midpoint between the medial and lateral malleoli pointing in the proximal direction, the z-axis was perpendicular to the y-axis oriented toward the most lateral point of the lateral tibial condyle, and the x-axis was perpendicular to both axes pointing anteriorly. For the patella, the origin of the coordinate system was located at the patella's center of mass, with the x, y, and z axes being parallel to those of the femoral coordinate system at full extension. Muscle fiber, tendon, and ligament bundle slack lengths were calibrated for each patient using the preosteophytic knee model configuration and remained unchanged in the osteophytic configuration. The same ligament mechanical properties, including stiffness and reference strain of each individual bundle, as those used in the original cadaveric model, were applied to both the osteophytic and preosteophytic models. Figure 3 depicts the osteophytic and preosteophytic musculoskeletal

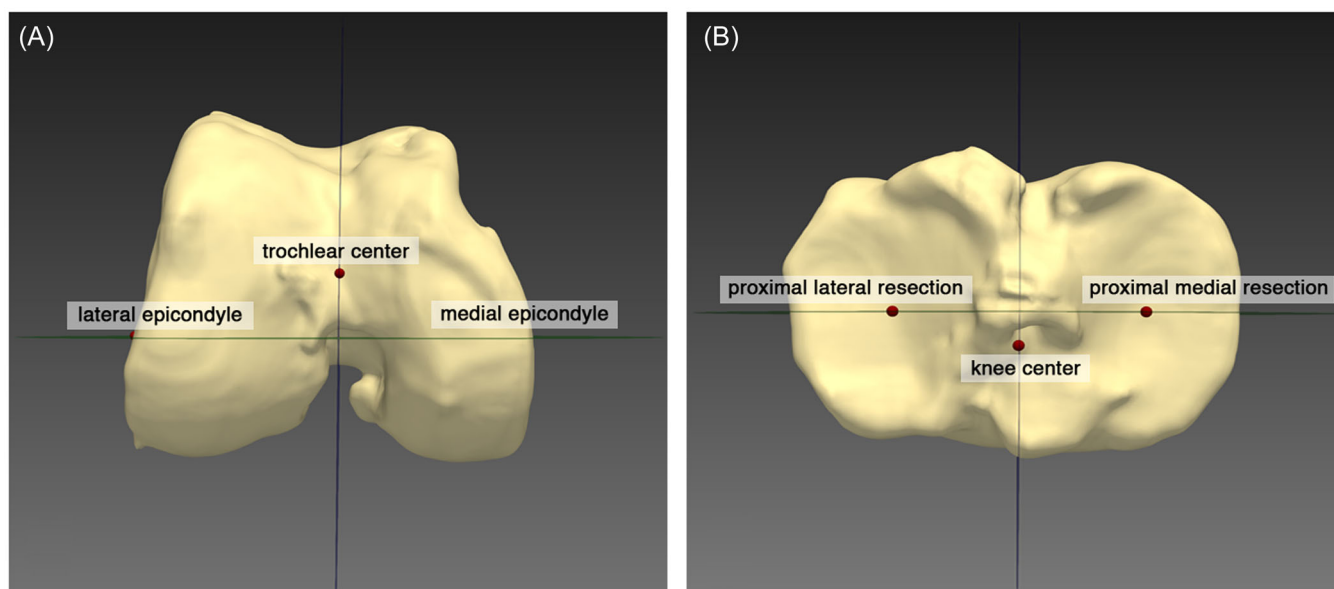


FIGURE 2 Partitioning of the (A) femoral and (B) tibial bone into anterior medial, anterior lateral, posterior medial, and posterior lateral compartments using orthogonal planes based on anatomical landmarks.

knee model of a single patient case with severe knee osteophytes. Figure 4 provides a schematic diagram that summarizes the main, sequential methodological steps involved in this study.

Strains of knee ligaments were reported during a knee extension simulation against gravity from 60° to 0°. Knee kinematics, namely

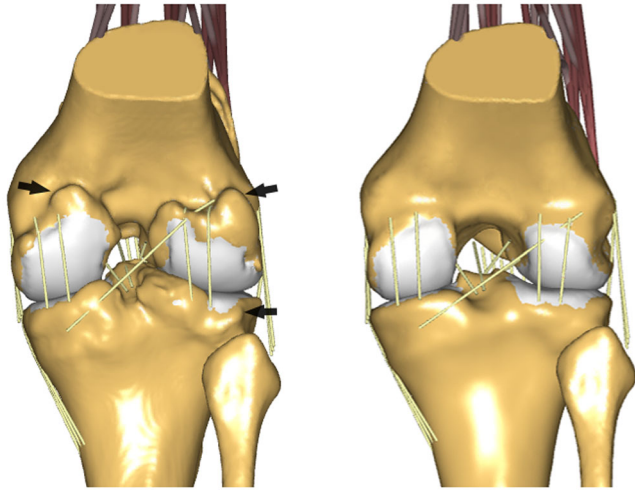


FIGURE 3 The musculoskeletal knee model of a single patient with severe knee osteophytes. From left to right, a close-up posterior view of the osteoarthritic knee model, presenting large posterior-compartment condylar and tibial osteophytes (black arrows) and severe narrowing of the joint space; and posterior view of the preosteophytic knee model, comprising the reconstructed osteophyte-free bone geometries.

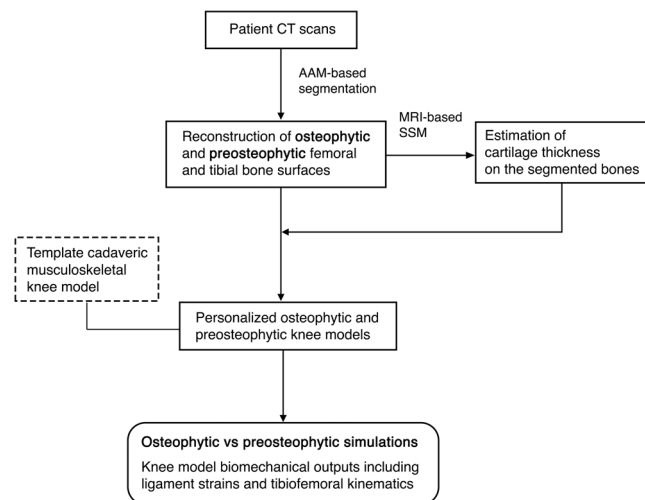


FIGURE 4 Schematic of the study's main methodological steps from patient's preoperative CT scans to active appearance model (AAM)-based segmentation of osteophytic and preosteophytic bones, and magnetic resonance image (MRI)-based statistical shape modeling (SSM) for estimation of cartilage thickness on the segmented bones; subsequently, personalization of a template musculoskeletal knee model using the patient-specific bone geometries and cartilage and, ultimately, biomechanical comparison of patient-specific osteophytic and preosteophytic knee models.

anterior–posterior (AP), lateral–medial (LM), and proximal–distal (PD) tibial translations, tibial external–internal (EI) rotation, and varus–valgus (VV), were calculated with both osteophytic and preosteophytic models for each patient throughout the simulation. Joint kinematics were estimated according to Grood and Suntay's joint coordinate system definition.²⁷ To address the first aim of this study, the differences between osteophytic and preosteophytic model predictions were quantified, by calculating the deviation in strain and kinematic variables at each flexion angle and, subsequently, by identifying the maximal value of those deviations across the range of motion. The Wilcoxon signed-rank test was used to evaluate the intragroup differences in ligament strains and knee kinematics between osteophytic and preosteophytic knees. To address the second research question, we examined the effect of osteophytic volume on ligament strains and knee kinematics using the Mann–Whitney *U* test for intergroup comparisons with Holm–Bonferroni correction. The significance level was set to 0.05. The relation of osteophyte volumetric differences, derived from the comparison of osteophytic and preosteophytic bones, and location of osteophytes with the resultant ligament strains and knee kinematics was evaluated using Pearson's correlation coefficient (*r*) interpreted according to a previously published stratification.²⁸ Specifically, coefficients <0.10 indicated a negligible correlation, while those in the range of 0.10–0.39 were considered weak; coefficients within 0.40–0.69 were interpreted as moderate, while values between 0.70 and 0.89 denoted strong correlations; finally, coefficients >0.9 denoted a very strong relationship between the variables.

3 | RESULTS

Strains in the ligaments were generally affected by the presence of osteophytes. The predicted strains comparing the osteophytic and preosteophytic knee models among all patients showed a median maximum deviation greater than 2.8% for cruciate ligaments, 1.3% for collateral ligaments, 2.9% and 1.7% for anterolateral and posterior ligamentous structures, respectively. Maximum deviations peaked at 15.7% in the ACL, 5.5% in the PCL, 8.9% in the dMCL, 5.6% in the sMCL, 5.7% in the LCL, 7.9% in the ALL, 11.7% in the OPL, and 28.0% in the PC, all found within the group of severe osteophytes except for the PCL (moderate osteophytes). Of these deviations, the PCL, dMCL, and sMCL peaks resulted from a higher strain in the preosteophytic model relative to the osteophytic knee model. Osteophytes had a marked effect on knee kinematics following the changes in the ligament strains. Compared to the preosteophytic models, the osteophytic knee models predicted kinematics with a median maximum deviation greater than 0.8 mm for translations and 1.4° for rotations overall patients. The largest median maximum deviation in kinematics was 1.6 mm in AP translation and 2.6° in EI rotation. Maximum kinematic deviations reached up to 3.7 mm for AP, 3.3 mm for LM, and 1.6 mm for PD translations, and up to 4.9° for IE and 4.0° for VV rotations within the group of patients with severe knee osteophytes. The maximum deviations occurred at different flexion

angles for each patient without a clear trend in the data, although we identified ranges applied to most patients. For AP and LM translations, the flexion angle at which maximum deviations occurred was within 20–40°, while for PD translation, it ranged from 0° to 30°; maximum deviations for EI and VV rotations were predominantly reported near extension in the range between 0° and 20°.

The effects on ligament strains exhibited large variability per patient, owing to the variable presence of osteophytes, but overall, the posterior ligamentous structures were more commonly affected than the other structures. In detail, the intragroup comparison showed a statistically significant difference in the strains of the ACL and PCL in mild osteophytic knees; PCL and LCL in moderate osteophytic knees; and ACL, PCL, OPL, and PC in the knees with severe osteophytes. As shown in Table 2, the sMCL, LCL, and PC strains in moderate osteophytic knees statistically significantly increased when compared to the group of mild osteophytes. Furthermore, strains in the sMCL, LCL, ALL, OPL, and PC were statistically significantly higher in severe osteophytic knees compared to mild osteophytic knees. The regression outcomes on the whole data set indicated negligible to strong correlations between ligament strains and osteophyte volumetric differences ranging from –0.004 to 0.711 (Figure 5). Strains in the ACL, dMCL, LCL, and PC were not significantly correlated with osteophyte volumes ($p < 0.05$); the strongest correlation was found for the ALL and OPL ($p < 0.001$). These results supported the need for multivariate analysis with respect to the osteophytic compartments (Figure 6). The changes in the kinematic patterns were variable among the patients and subject to the interaction of contact surfaces. There were no intragroup differences in knee kinematics between osteophytic and preosteophytic knees, except for EI rotation which was statistically significantly higher in the osteophytic knees within the group of moderate osteophytes ($p = 0.043$). The results of the comparison of mild, moderate, and severe osteophyte groups are displayed in Table 3.

The LM translation in moderate osteophytic knees was statistically significantly higher compared to mild osteophytic cases. Severe osteophytic knees showed significantly increased LM translation and EI rotation when compared to the group of mild osteophytes. The regression analysis revealed weak to moderate correlations between kinematics and osteophyte volumetric differences ($r = 0.171–0.670$) (Figure 7). The AP translation and EI rotation showed a significant correlation with osteophyte volumes with an r -value of 0.444 ($p = 0.044$) and 0.670 ($p < 0.001$), respectively. Correlation coefficients between knee kinematics and osteophyte volumetric differences per compartment are depicted in Figure 6.

4 | DISCUSSION

This study investigated the effects of osteophytes on ligament strains and consequent knee kinematics comparing osteophytic knees sorted into different osteophyte stages with their respective preosteophytic reconstruction. The effects were variable among the patients, depending on the osteophyte's location and the interaction of contact surfaces or ligament wrapping with the osteophyte. This variability explains the variable manifestation of knee OA and the formation of osteophytes among different patients.

Severe osteophytes generally affected the ligament strains in a relevant manner. One of the most important findings of this study was that severe osteophytic knees substantially strained the OPL and PC structures, exhibiting peak strain deviations from the preosteophytic situation, which were higher than the clinically acceptable threshold of 5.1%, as previously described.^{29,30} Since the lateral aspect of the capsule attaches superiorly to the cortex of the posterior femoral condyle and the proximal lateral attachment of the OPL expands diagonally over the capsular structure, the presence of large posterolateral condylar osteophytes may result in tightening of the capsular

TABLE 2 Effect of mild, moderate, and severe osteophytes on knee ligament strains.

	Mild osteophytes	Moderate osteophytes	Severe osteophytes	<i>p</i> Value Mild vs. moderate	Moderate vs. severe	Mild vs. severe
<i>Ligament strains^a</i>						
ACL	3.15 [1.44, 6.30]	5.82 [3.23, 9.17]	3.14 [2.75, 11.02]	0.110	0.565	0.406
PCL	1.97 [1.05, 3.85]	3.78 [2.82, 4.31]	2.33 [1.02, 4.21]	0.144	0.142	0.482
dMCL	2.94 [2.21, 3.92]	3.64 [2.59, 5.00]	7.72 [6.30, 8.31]	0.338	0.073	0.054 ^b
sMCL	0.99 [0.87, 1.66]	2.78 [1.84, 3.36]	2.53 [1.74, 3.20]	0.027	0.565	0.026
LCL	0.67 [0.23, 1.17]	1.40 [0.87, 2.50]	2.82 [1.30, 4.36]	0.050	0.277	0.027
ALL	1.68 [1.19, 2.59]	2.86 [1.89, 3.03]	4.35 [3.55, 6.56]	0.110	0.012	0.006
OPL	1.18 [0.91, 1.72]	1.36 [1.28, 1.93]	3.44 [2.58, 5.05]	0.450	0.006	0.006
PC	2.13 [1.21, 2.55]	5.14 [2.96, 8.00]	8.06 [5.86, 20.02]	0.022	0.073	0.006

Note: Data are presented as median [interquartile range]. Bold figures indicate significance after Holm–Bonferroni correction.

^aStrain is expressed as a percent strain.

^bDifference is no longer significant after Holm–Bonferroni correction.

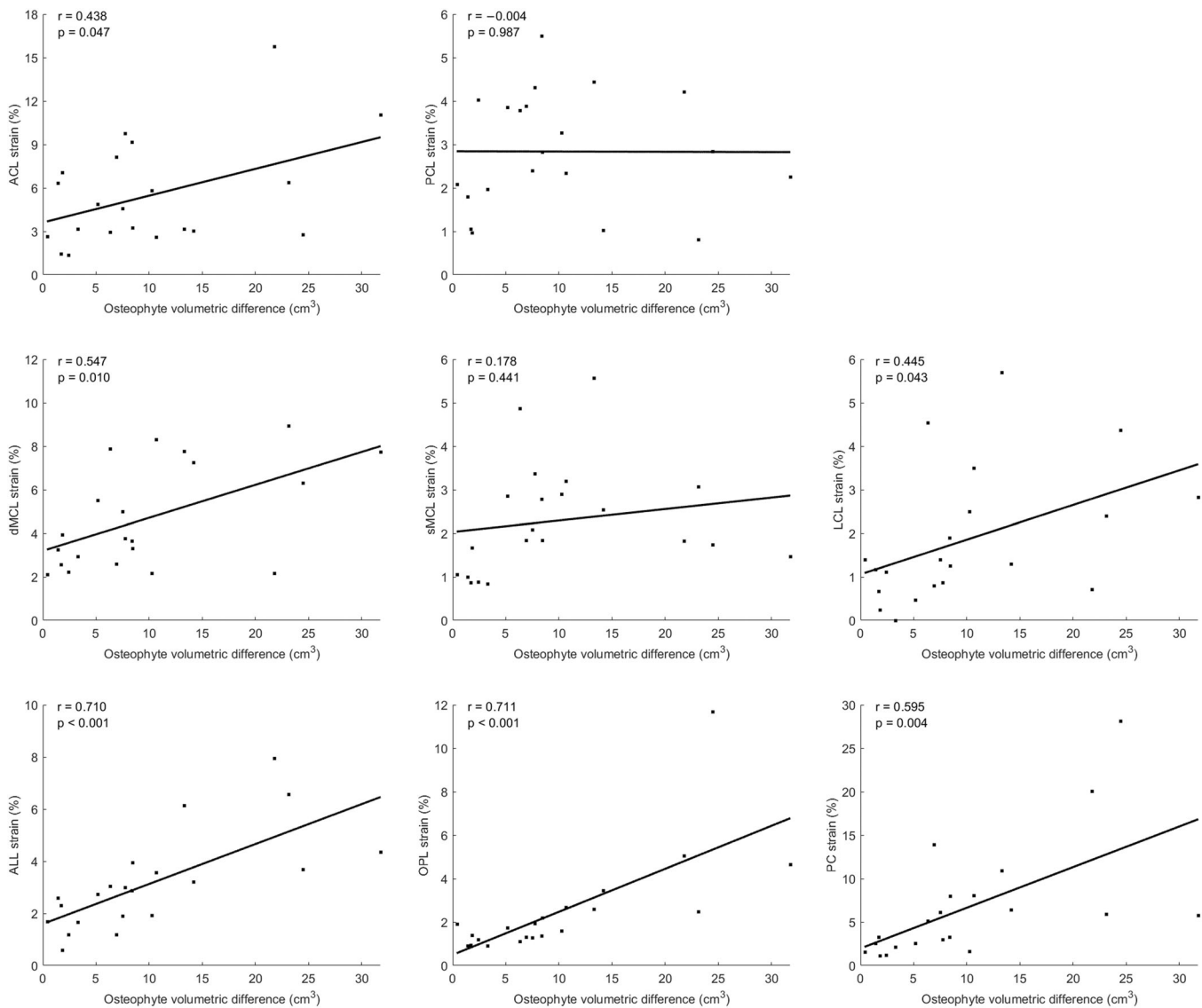


FIGURE 5 Correlation between knee ligament strains and osteophyte volumetric differences. Osteophyte volumetric difference refers to the sum of the differences in volume between the osteophytic and preosteophytic femoral and tibial bone surfaces. Mild osteophytes range from 0 to 5 cm³, moderate osteophytes from 5 to 10 cm³, and severe osteophytes from 10 cm³ onwards.

ligaments due to their wrapping around these osteophytic outgrowths, as confirmed by our multivariate, compartmental analysis (Figure 7). This finding is consistent with that of Leie et al.³¹ who demonstrated that large posterior femoral osteophytes can cause a tenting effect on the posterior joint capsule. Additionally, we found that greater strains in the OPL were strongly correlated with greater PC strains (Figure 6), as expected due to their anatomical intersection. Straining of these ligamentous structures might be related to the statistically significantly increased EI rotation in severe osteophytic knees. Peak deviations in EI rotation among the knees with severe osteophytes predominantly occurred between 0° and 20°, but this was not the case for all patients. The fibers of the PC are typically tense in knee extension, and this would further increase in the presence of the OPL, consequently altering EI rotation at low flexion angles. One anatomical study suggested that the OPL functions as a rotational stabilizer

preventing excessive tibial external rotation due to the horizontal component of the diagonal bundle's force.³² However, if the OPL is subject to excessive strain or is structurally damaged, this stabilizing effect may be reduced, leading to increased rotational motion. In this study, we did not confirm an association between the OPL strain and EI rotation. Another reason for the increased EI rotation angle might be related to the absence of the posterior oblique ligament in the knee model, which has been previously confirmed to primarily stabilize the joint against internal rotation during early flexion (0–30°).³³ Furthermore, the simplified patellar model used in the current study could potentially contribute to the increased EI rotation angles. Previous research has shown that increased external rotation of the tibia relative to the femur is associated with a laterally tilted patella,³⁴ which could be due to the presence of trochlear osteophytes. Another finding worth discussing is that severe osteophytic knees considerably

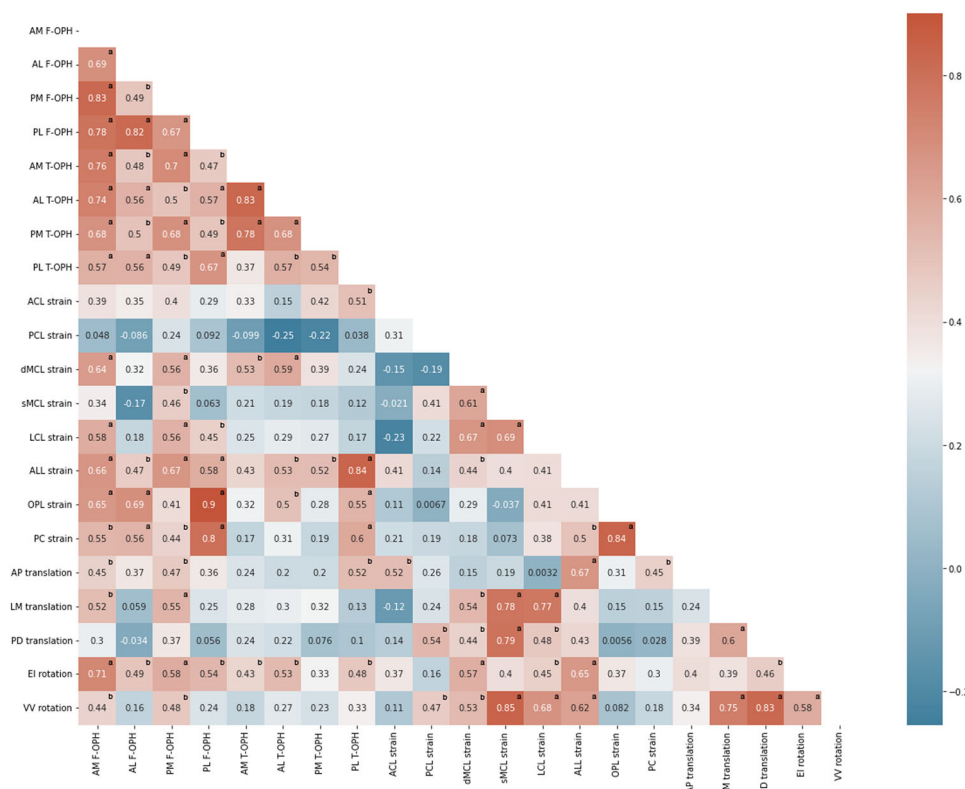


FIGURE 6 Multivariate correlation matrix displaying Pearson's correlation coefficients for knee kinematic variables and ligament strains in relation to the osteophytic compartments. Positive correlations are colored in red, while negative correlations are in blue. Color intensity is proportional to the correlation-coefficient value. AL, anterolateral; AM, anteromedial; AP, anterior–posterior; EI, external–internal; F-OPH, femoral osteophytes; LM, lateral–medial; PD, proximal–distal; PL, posterolateral; PM, posteromedial; T-OPH, tibial osteophytes; VV, varus–valgus. ^aCorrelation is significant at the 0.01 level. ^bCorrelation is significant at the 0.05 level.

TABLE 3 Effect of mild, moderate, and severe osteophytes on knee kinematics.

	Mild osteophytes	Moderate osteophytes	Severe osteophytes	<i>p</i> Value Mild vs. moderate	Moderate vs. severe	Mild vs. severe
<i>Knee kinematics</i>						
Translations (mm)						
AP	0.99 [0.62, 1.99]	1.47 [1.04, 2.08]	1.95 [1.62, 2.24]	0.142	0.110	0.064
LM	0.84 [0.62, 1.03]	1.55 [1.16, 2.83]	1.84 [1.74, 1.96]	0.050	0.655	0.027
PD	0.58 [0.40, 0.68]	0.78 [0.54, 1.07]	0.80 [0.73, 0.92]	0.141	0.654	0.105 ^a
Rotations (°)						
EI	2.06 [1.27, 2.41]	2.93 [1.73, 3.59]	3.44 [2.61, 4.78]	0.450	0.450	0.018
VV	0.66 [0.36, 1.37]	1.87 [1.16, 2.46]	1.61 [1.40, 2.77]	0.075 ^a	0.655	0.075 ^a

Note: Data are presented as median [interquartile range]. Bold figures indicate significance after Holm–Bonferroni correction.

^aDifference is no longer significant after Holm–Bonferroni correction.

increased the strain in the ACL compared to their preosteophytic counterparts, with maximum deviations well above the predetermined damage threshold²⁹; exceeding the ACL's yield region³⁵ is clinically relevant and could eventually lead to a limited range of AP motion and pain. The uncertain choice of the ligament reference strains may have

contributed to this nonphysiological finding, as it is possible the pretensions of the ACL bundles were excessively high for some patients. Earlier research has identified intercondylar notch stenosis due to osteophytes, generating a shear force on the ACL and, eventually, an increase in the bundles' strain.³⁶ Although our model

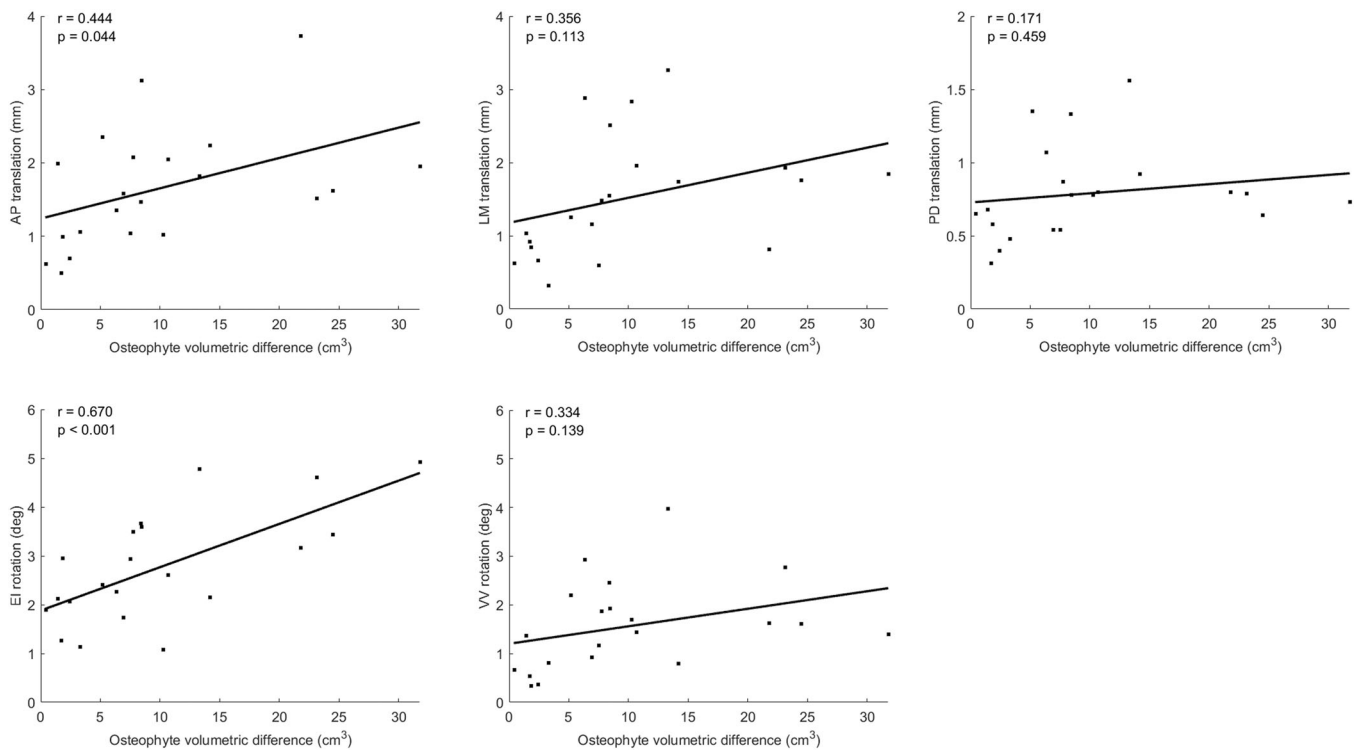


FIGURE 7 Correlation between knee kinematics and osteophyte volumetric differences. Osteophyte volumetric difference refers to the sum of the differences in volume between the osteophytic and preosteophytic femoral and tibial bone surfaces. Mild osteophytes range from 0 to 5 cm³, moderate osteophytes from 5 to 10 cm³, and severe osteophytes from 10 cm³ onwards.

accounted for the interaction of the ACL bundles and the interfering osteophytes at the intercondylar eminence of the tibial plateau, allowing the ligament to wrap around the osteophytic surface, we did not consider the effect of the femoral notch width on the bundles' strain. Our multivariate analysis showed a weak or moderate correlation between anterior and posterior compartment osteophytes and the ACL strain deviations. This may explain the similar AP translation within the three osteophyte groups. The cruciate ligaments are primary restraints to anterior and posterior displacement and the small change to their strains would logically affect marginally the AP translation. In the medial collateral ligamentous structures, we found strain deviations peaked at 8.9% between osteophytic and preosteophytic knees, which cannot be disregarded clinically.³⁷ Provenzano et al.²⁹ have previously detected the onset of fiber plastic deformation at 5.1% strain in the medial collaterals; subfailure strains above this damage threshold may potentially induce complete or nearly complete disruption of the ligament, ultimately resulting in increased laxity on the medial side. The dMCL and sMCL strains were weakly or moderately correlated with the volume of anteromedial and posteromedial compartment osteophytes. We measured larger osteophyte volumes at the peripheral margins of the medial joint articulation, and thus, the wrapping effect around the attachment sites of these ligaments was expected to be relatively small. These outcomes are partly contradictory to the ideas of Mihalko et al.³⁸ who suggested that the presence of medial-compartment osteophytes can significantly tighten the ligamentous structures of the medial soft-tissue sleeve, recommending their

removal to achieve a balanced flexion and extension gap in varus knees. Based on these findings, we can infer that statistically significant straining of the sMCL in moderate and severe osteophytic knees is likely to be related to kinematic deviations. There was a strong correlation between the sMCL strain and VV rotation, which further supports previous observations linking osteophyte size with knee alignment at the side of the osteophytes.³⁹ Although the observed differences in VV rotation among the three osteophyte groups were not statistically significant, this does not imply the absence of intergroup differences. Interestingly, the ALL that overlaps the proximal LCL bundles showed a substantial increase in severe osteophytic knees (Table 2), with strain deviations peaking at 7.9% compared to the preosteophytic state, which can be of clinical importance, yet we observed strain magnitudes within the ultimate strain region.⁴⁰ There was a strong correlation of the ALL with posterolateral tibial osteophyte volumes (Figure 6). Since the osteophytes at the lateral tibial plateau predominantly extend upwards,⁴¹ we speculate an increase in the varus rotation angle, thus inducing straining of the ALL (Figure 6). Another possible explanation might be that the compartment-specific osteophytes strained the posterior ligamentous structures, which consequently forced the tibia to rotate internally; therefore, there was an increase in the ALL strain, which is known to be an internal rotation restraint. Clinically, it has been suggested that the ALL contributes to protecting the ACL from injury mechanisms induced by tibial internal rotation.⁴² The association between the ALL and ACL was moderately reflected in our multivariate analysis outcomes.

This simulation study explores the biomechanical consequences of knee osteophytes and thoroughly examines the association of compartment-specific osteophyte volumes with knee ligament strain and kinematic deviations, which is not achievable in clinical trials. A major strength of this study was the novel methodology employed that combined statistical modeling to identify the preosteophytic knee bone shapes with musculoskeletal simulations to assess the biomechanical impact of knee osteophytes and predict the consequences of their removal. These simulations could potentially provide relevant quantitative insights for orthopaedic surgeons during the preoperative planning for total knee arthroplasty, toward reinstating as closely as possible the physiological knee biomechanics.

This study had some limitations. First, the model predictions could not be directly validated, reiterating the importance of an *in vivo* assessment of the ligament and bone interaction with the osteophytes. Besides, the simplified 1-degree-of-freedom patellofemoral joint might have influenced the accuracy of the model's kinematic predictions,⁴³ as the complex interaction between the tibiofemoral and patellofemoral joints is largely dependent on the surrounding soft tissues. With regard to the structure, the model excluded the menisci, functioning to maintain joint congruity, which could have induced alterations in the tibiofemoral kinematics. Additionally, the ligament models were not patient-specific and their mechanical properties, including stiffness and reference strain, were derived from the literature. Using identical ligament properties in the subject-specific models ensured equal levels of uncertainty in their predictions and, consequently, enabled us to isolate the effect of osteophytes on the joint's biomechanics. Nevertheless, there might still be uncertainties in the model predictions resulting from measurement errors or interpatient anatomical variations, which emphasizes the importance of subjecting the models to a thorough verification, validation, and uncertainty quantification process to assess the accuracy and reliability of the model outputs before patient-specific application. The reported findings pertain only to a knee flexion-extension activity. In principle, it would be possible to investigate also other motor tasks, such as squatting or chair-rising, as previously described,⁴⁴ yet the selected activity can be performed *intra-operatively* and is relevant to assess the appropriate tensioning of the soft tissues, which is important for achieving an adequately balanced motion during flexion and extension. Besides, the observed differences between the osteophytic and preosteophytic models are expected to persist, irrespective of the activity performed, since they are inherent to the presence of osteophytes and their interference with the relevant soft tissues. We should also note that the knee motion was simulated without any applied external loads, as these may vary among patients and it was unfeasible to measure in this study. Although it is possible that the strain and kinematic differences between the osteophytic and preosteophytic knee in an unloaded state may persist under loading conditions, the validity of this assumption remains to be proven. Another limitation of this study was that the mechanical properties of the soft tissues remained unmodified between the osteophytic and preosteophytic models, whereas, in reality, these are likely to

change over time secondary to OA.⁴⁵ The timeline of such changes, however, was difficult to predict in this study due to the variable nature of the soft-tissue remodeling process, which may depend on the size and location of osteophytes and the extent of their interference with the surrounding soft tissues. Our findings should therefore be interpreted on the basis of this assumption with the recognition that a future study should incorporate soft-tissue models reflective of the patient-specific changes owing to disease progression. Finally, this study did not evaluate alterations in the patellofemoral joint and the potential effects of osteophytes on the patella's functioning. Nonetheless, the strain of the patellar tendon during the simulated movement was found to be relatively low and, consequently, there was a minimal effect of the patellofemoral joint on the knee mechanics.

In summary, the presence of osteophytes in OA knees induced clinically relevant changes in the ligament strains and kinematics compared to their corresponding preosteophytic state. These changes were variable and patient-specific, indicating a dependency on the osteophyte volume and location and the interaction of the ligamentous structures with the osteophytic compartment. The suggested approach introduces a quantitative framework, providing data on the biomechanical impact of knee osteophytes, as well as the potential effects of their removal. These data can assist orthopaedic surgeons during the preoperative phase of total knee arthroplasty, revealing the need of conducting biomechanical preoperative planning with osteophytes removed, toward restoring the physiological knee's biomechanical conditions.

AUTHOR CONTRIBUTIONS

Periklis Tzanetis, René Fluit, and Nico Verdonshot designed the study. Kevin de Souza and Seonaid Robertson acquired and preprocessed the data. Periklis Tzanetis processed, analyzed, and interpreted the data. René Fluit assisted in developing the methodology and data analysis framework. Periklis Tzanetis prepared the draft of the manuscript. Periklis Tzanetis, René Fluit, and Nico Verdonshot critically revised the manuscript. Nico Verdonshot and Bart Koopman coordinated the research activities. All authors have read and approved the submitted manuscript.

ACKNOWLEDGMENTS

This research was funded by Stryker European Operations Ltd., Ireland. Kevin de Souza is an employee of Stryker, and holds stock and stock options in Stryker Corporation. Seonaid Robertson is an employee of Stryker. We acknowledge Eric Garling (Stryker, Montreux, Switzerland), José-Luis Moctezuma (Stryker, Freiburg, Germany), and Daniele De Massari (Stryker, Amsterdam, The Netherlands) for their help in the acquisition of data. Furthermore, we are thankful to Michael Kohnen (Stryker, Freiburg, Germany) for his kind assistance in using the image segmentation software.

ORCID

Periklis Tzanetis  <http://orcid.org/0000-0001-6396-9896>

René Fluit  <http://orcid.org/0000-0002-2450-7071>

REFERENCES

1. Tozawa R, Ogawa Y, Minamoto Y, et al. Possible role of MRI-detected osteophytes as a predictive biomarker for development of osteoarthritis of the knee: a study using data from the osteoarthritis initiative. *Osteoarthritis Cartilage Open*. 2021;3:100200.
2. van der Kraan PM, van den Berg WB. Osteophytes: relevance and biology. *Osteoarthritis Cartilage*. 2007;15:237-244.
3. Rabelo GD, vom Scheidt A, Klebig F, et al. Multiscale bone quality analysis in osteoarthritic knee joints reveal a role of the mechanosensory osteocyte network in osteophytes. *Sci Rep*. 2020;10:673.
4. Dayal N, Chang A, Dunlop D, et al. The natural history of anteroposterior laxity and its role in knee osteoarthritis progression. *Arthritis Rheum*. 2005;52:2343-2349.
5. Wong SHJ, Chiu KY, Yan CH. Review article: osteophytes. *J Orthop Surg*. 2016;24:403-410.
6. Markhardt BK, Li G, Kijowski R. The clinical significance of osteophytes in compartments of the knee joint with normal articular cartilage. *Am J Roentgenol*. 2018;210:W164-W171.
7. Holst DC, Dennis DA. Pearls: early removal of posterior osteophytes in TKA. *Clin Orthop Relat Res*. 2018;476:684-686.
8. Felson DT. Osteophytes and progression of knee osteoarthritis. *Rheumatology*. 2005;44:100-104.
9. Yagishita K, Muneta T, Ikeda H. Step-by-step measurements of soft tissue balancing during total knee arthroplasty for patients with varus knees. *J Arthroplasty*. 2003;18:313-320.
10. Motesharei A, Batailler C, De Massari D, Vincent G, Chen AF, Lustig S. Predicting robotic-assisted total knee arthroplasty operating time: benefits of machine-learning and 3D patient-specific data. *Bone Joint Open*. 2022;3:383-389.
11. Vincent G, Wolstenholme C, Scott I, Bowes M. Fully automatic segmentation of the knee joint using active appearance models. *Med Image Anal*. 2010;1:224-230.
12. Bowes MA, Kacena K, Alabas OA, et al. Machine-learning, MRI bone shape and important clinical outcomes in osteoarthritis: data from the osteoarthritis initiative. *Ann Rheum Dis*. 2021;80:502-508.
13. Marra MA, Vanheule V, Fluit R, et al. A subject-specific musculoskeletal modeling framework to predict in vivo mechanics of total knee arthroplasty. *J Biomech Eng*. 2015;137:1-12.
14. Oussedik S, Scholes C, Ferguson D, Roe J, Parker D. Is femoral component rotation in a TKA reliably guided by the functional flexion axis? *Clin Orthop Relat Res*. 2012;470:3227-3232.
15. Skipper Andersen M, De Zee M, Damsgaard M, Nolte D, Rasmussen J. Introduction to force-dependent kinematics: theory and application to mandible modeling. *J Biomech Eng*. 2017;139:091001.
16. Rowe PJ, Myles CM, Walker C, Nutton R. Knee joint kinematics in gait and other functional activities measured using flexible electrogoniometry: how much knee motion is sufficient for normal daily life? *Gait Posture*. 2000;12:143-155.
17. Thelen DG, Won Choi K, Schmitz AM. Co-simulation of neuromuscular dynamics and knee mechanics during human walking. *J Biomech Eng*. 2014;136:021033.
18. Carbone V, Fluit R, Pellikaan P, et al. TLEM 2.0—a comprehensive musculoskeletal geometry dataset for subject-specific modeling of lower extremity. *J Biomech*. 2015;48:734-741.
19. LaPrade RF, Ly TV, Wentorf FA, Engebretsen AH, Johansen S, Engebretsen L. The anatomy of the medial part of the knee. *TJ Bone Joint Surg Am Vol*. 2007;89:2000-2010.
20. Blankevoort L, Kuiper JH, Huiskes R, Grootenboer HJ. Articular contact in a three-dimensional model of the knee. *J Biomech*. 1991;24:1019-1031.
21. Dejtiar DL, Dzialo CM, Pedersen PH, Jensen KK, Fleron MK, Andersen MS. Development and evaluation of a subject-specific lower limb model with an eleven-degrees-of-freedom natural knee model using magnetic resonance and biplanar x-ray imaging during a quasi-static lunge. *J Biomech Eng*. 2020;142:061001.
22. Abulhasan J, Snow M, Anley C, Bakhsh M, Grey M. An extensive evaluation of different knee stability assessment measures: a systematic review. *J Funct Morphol Kinesiol*. 2016;1:209-229.
23. Cannon WD. Use of arthrometers to assess knee laxity and outcomes. *Sports Med Arthrosc*. 2002;10:191-200.
24. Kohn MD, Sassoon AA, Fernando ND. Classifications in brief: Kellgren-Lawrence classification of osteoarthritis. *Clin Orthop Relat Res*. 2016;474:1886-1893.
25. Hunter DJ, Bowes MA, Eaton CB, et al. Can cartilage loss be detected in knee osteoarthritis (OA) patients with 3–6 months' observation using advanced image analysis of 3T MRI? *Osteoarthr Cartil*. 2010;18:677-683.
26. Williams TG, Holmes AP, Waterton JC, et al. Anatomically corresponded regional analysis of cartilage in asymptomatic and osteoarthritic knees by statistical shape modelling of the bone. *IEEE Trans Med Imaging*. 2010;29:1541-1559.
27. Grood ES, Suntay WJ. A joint coordinate system for the clinical description of three-dimensional motions: application to the knee. *J Biomech Eng*. 1983;105:136-144.
28. Schober P, Boer C, Schwarte LA. Correlation coefficients: appropriate use and interpretation. *Anesth Analg*. 2018;126:1763-1768.
29. Provenzano PP, Heisey D, Hayashi K, Lakes R, Vanderby R. Subfailure damage in ligament: a structural and cellular evaluation. *J Appl Physiol*. 2002;92:362-371.
30. Guo Z, Freeman JW, Barrett JG, De Vita R. Quantification of strain induced damage in medial collateral ligaments. *J Biomech Eng*. 2015;137:071011.
31. Leie MA, Klasan A, Oshima T, et al. Large osteophyte removal from the posterior femoral condyle significantly improves extension at the time of surgery in a total knee arthroplasty. *J Orthop*. 2020;19:76-83.
32. Wu XD, Yu JH, Zou T, et al. Anatomical characteristics and biomechanical properties of the oblique popliteal ligament. *Sci Rep*. 2017;7:42698.
33. D'Ambrosi R, Corona K, Guerra G, Rubino M, Di Feo F, Ursino N. Biomechanics of the posterior oblique ligament of the knee. *Clin Biomech*. 2020;80:105205.
34. Wu G, Cao Y, Song G, et al. The increased tibiofemoral rotation: a potential contributing factor for patellar maltracking in patients with recurrent patellar dislocation. *Orthop Surg*. 2022;14:1469-1475.
35. Butler DL, Kay MD, Stouffer DC. Comparison of material properties in fascicle-bone units from human patellar tendon and knee ligaments. *J Biomech*. 1986;19:425-432.
36. Lee GC, Cushner FD, Vigorita V, Scuderi GR, Insall JN, Scott WN. Evaluation of the anterior cruciate ligament integrity and degenerative arthritic patterns in patients undergoing total knee arthroplasty. *J Arthroplasty*. 2005;20:59-65.
37. Delpont H, Labey L, Innocenti B, De Corte R, Vander Sloten J, Bellemans J. Restoration of constitutional alignment in TKA leads to more physiological strains in the collateral ligaments. *Knee Surg Sports Traumatol Arthrosc*. 2015;23:2159-2169.
38. Mihalko WM, Saleh KJ, Krackow KA, Whiteside LA. Soft-tissue balancing during total knee arthroplasty in the varus knee. *J Am Acad Orthop Surg*. 2009;17:766-774.
39. Ishii Y, Noguchi H, Sato J, et al. Size of medial knee osteophytes correlates with knee alignment but not with coronal laxity in patients with medial knee osteoarthritis. *J Orthop Res*. 2020;38:639-644.
40. Smeets K, Slane J, Scheyls L, Claes S, Bellemans J. Mechanical analysis of extra-articular knee ligaments. *Knee*. 2017;24:949-956.
41. Nagaosa Y. Characterisation of size and direction of osteophyte in knee osteoarthritis: a radiographic study. *Ann Rheum Dis*. 2002;61:319-324.
42. Blanke F, Boljen M, Lutter C, Oehler N, Tischer T, Vogt S. Does the anterolateral ligament protect the anterior cruciate ligament in the most common injury mechanisms? A human knee model study. *Knee*. 2021;29:381-389.
43. Guan S, Gray HA, Thomeer LT, Pandy MG. A two-degree-of-freedom knee model predicts full three-dimensional tibiofemoral

- and patellofemoral joint motion during functional activity. *Ann Biomed Eng.* 2022;51:493-505.
44. Tzanetis P, Marra MA, Fluit R, Koopman B, Verdonschot N. Biomechanical consequences of tibial insert thickness after total knee arthroplasty: a musculoskeletal simulation study. *Applied Sciences.* 2021;11:2423.
45. Fishkin Z, Miller D, Ritter C, Ziv I. Changes in human knee ligament stiffness secondary to osteoarthritis. *J Orthop Res.* 2002;20:204-207.

How to cite this article: Tzanetis P, de Souza K, Robertson S, Fluit R, Koopman B, Verdonschot N. Numerical study of osteophyte effects on preoperative knee functionality in patients undergoing total knee arthroplasty. *J Orthop Res.* 2024;1-12. doi:10.1002/jor.25850